Vertical stability of anchored concrete soldier-pile walls in clay

By N. M. da C. Guerra[1], A. S. Cardoso[2], M. Matos Fernandes[3] & A. Gomes Correia[4]

Abstract

The problem of vertical stability in flexible anchored retaining walls is analyzed and the pattern of the behavior under conditions of poor vertical support is described, on the basis of results from case-histories, small-scale tests and numerical modeling. The possibility of shear stress mobilization in the soil-to-wall interface of anchored concrete soldier-pile retaining walls is discussed. A finite element procedure to model excavations supported by soldier-pile retaining walls is described and applied to a numerical case study. Finite element analyses are performed, emphasizing the consequences of vertical instability due to buckling of the soldier-piles and the role of interface resistance in vertical equilibrium. The understanding of some results of the numerical analyses, which are highly influenced by the complexity of the interaction between the different parts of the structure, is obtained by re-assessing the vertical equilibrium issue in the light of limit analysis. This approach makes it possible to estimate the pile resistance corresponding to the limit situation of excavation collapse. The finite element model is used to confirm this resistance. Some conclusions are drawn.

1 INTRODUCTION

Deep excavations in urban areas are sometimes supported by anchored soldier-pile walls, often called Berlin-type walls. In most cases these are used just as a temporary structure, comprising steel piles inserted in vertical holes drilled at the border of the excavation area with timber

[1]Assistant Professor, Technical University of Lisbon - IST, Civil Engng. and Archit. Dep., Av. Rovisco Pais 1, 1049-001 Lisbon, Portugal, Fax: +351.218418427; Tel.: +351.218418419; E-mail: nguerra@civil.ist.utl.pt

[2]Professor, University of Oporto - FEUP, Civil Engng. Dep., R. Dr. Roberto Frias, 4200-465 Oporto, Portugal, Fax: +351.225081446, Tel.: +351.225081945, E-mail: scardoso@fe.up.pt

[3]Professor, University of Oporto - FEUP, Civil Engng. Dep., R. Dr. Roberto Frias, 4200-465 Oporto, Portugal, Fax: +351.225081446, Tel.: +351.225081947, E-mail: mfern@fe.up.pt

[4]Professor, University of Minho, Civil Engng. Dep., Azurém, 4800-058 Guimarães, Portugal, Fax: +351.253510217, Tel.: +351.253510200, E-mail: agc@civil.uminho.pt

Keywords: Anchored retaining wall, concrete soldier pile walls, vertical equilibrium, finite elements, limit analysis, soil-to-wall interface shear forces

lagging between pile flanges. Under certain geotechnical conditions, a permanent wall can be constructed by a similar process if cast-in-place reinforced concrete panels are used instead of timber lagging. Figure 1 illustrates the typical construction sequence of a concrete soldier-pile wall.

This paper presents some results of a joint research project between the Technical University of Lisbon and the University of Oporto, on the vertical stability of anchored concrete soldier-pile walls (Guerra, 1999). The project was prompted by the occurrence of a number of incidents with such structures, involving substantial movements of the retaining wall and supported ground and some damage to the vicinity. The interpretation of these events revealed insufficient resistance of the soldier-piles to vertical loads. In some cases, structural failure by pile buckling was observed.

Figure 2 shows the forces involved in the vertical equilibrium in soldier-pile walls. Vertical equilibrium requires that the following equation be verified:

$$W_w + \sum A sin\beta = N_{pile} + F_l \tag{1}$$

where:

- W_w is the weight of the wall per unit length;
- $\sum A sin\beta$ is the vertical force applied by the anchors per unit length of the wall;
- N_{pile} is the reaction mobilized on the soldier-piles per unit length of the wall;
- F_l is the shear force mobilized at the soil-to-wall interface per unit length of the wall, which can be written as:

  $$F_l = p c_a H_w \tag{2}$$

  where:

  - p is the mobilized ratio of the interface resistance, which can assume values between -1 (full downwards mobilization) and $+1$ (full upwards mobilization);
  - c_a is the soil-to-wall resistance (adhesion);
  - H_w is the wall height at each excavation level and, therefore, the corresponding length of the soil-to-wall interface.

The aim of the paper is to clarify the role of shear forces at the soil-to-wall interface in the vertical equilibrium of the structure. The magnitude (and direction) of these forces will naturally affect, to a large extent, the vertical loads to be carried by the soldier-piles. A good performance of the retaining structure will then require that these loads be less than the structural resistance of the piles as well as the bearing capacity of their foundation.

The paper contains three main sections:

- a review of the literature, collecting data from case histories and results from small-scale lab tests and from numerical studies;
- the description and discussion of a set of finite element analyses of a simplified numerical case study;
- a limit analysis approach to the problem taking into account the conclusions of the f. e. results.

In the closing section some conclusions are drawn.

2 LITERATURE SURVEY

Some clarification is required concerning the distinct types of flexible retaining structures. The walls whose construction is (mostly) complete before excavation is carried out will be called embedded walls. These walls, such as sheet-pile, diaphragm or concrete pile walls, have two faces (back and front faces) in contact with the ground. On the contrary, soldier-pile walls are partially constructed following the progress of the excavation. So, in concrete soldier-pile walls shear force interaction with the ground is just done through the back wall face.

Table 1 summarizes the incidents and accidents related with vertical equilibrium of anchored flexible retaining walls reported in the literature. They refer to embedded and to both conventional and concrete soldier-pile walls. The last four lines of the table correspond to the incidents and accidents mentioned in the previous section.

Very useful indications regarding vertical stability can also be extracted from studies by Hanna and Matallana (1970), Plant (1972) and Hanna and Abu-Taleb (1972) on small-scale tests of tied-back walls in sand, although their main focus is on other aspects of the behavior of such structures. In some of the tests, the excavation reached the base of the wall, thereby

aggravating the stability conditions in relation to vertical actions. The behavior observed under such circumstances was consistent with the above-mentioned case histories; there was a sudden increase of both components of wall displacement accompanied by large settlements behind the wall and by drop of the anchor loads.

The vertical stability of anchored walls in clay has been analyzed by Matos Fernandes et al. (1993). The authors present f. e. analyses of the failure of a sheet-pile wall reported by Broms and Stille (1976) (see Table 1), highlighting the evolution of the mobilization of shear stresses on the front and back wall faces when the system approaches failure by loss of vertical equilibrium.

This brief literature survey permits to depict the overall pattern of behavior of anchored retaining walls (both embedded and soldier-pile walls) under marginal stability conditions in relation to vertical loading, regardless of the type of soil, clay or sand:

- the wall experiences large settlements together with considerable lateral displacements;
- large horizontal and vertical displacements occur at the ground surface, reaching their maximum just close to the cut face;
- (in most cases) anchor forces exhibit important reductions.

Additionally, an interesting feature is revealed by the results of the previously mentioned small-scale tests and of finite element analyses: the upward shear forces induced at the back wall face by the very large settlements of embedded walls prior to the loss of vertical equilibrium, do not always represent a large fraction of the resistance of the interface. For example, at the back wall face, Plant (1972) reports mobilized soil (sand)-wall (aluminium) friction angles of a maximum of 11^o for an anchor inclination of 30^o; but when the anchor inclination was increased to 45^o, although the wall settlement was three times higher, the mobilized friction angle was only 5^o. This result will be further discussed in the following sections for the case of concrete soldier-pile walls.

3 FINITE ELEMENT ANALYSES

3.1 Description of the numerical case study

A 2D finite element geotechnical code (Cardoso, 1987; Almeida e Sousa, 1998; Guerra, 1999) was used. Some details of the simulation are provided in Appendix I since finite element analysis

of excavations supported by concrete soldier-pile walls is not common in the literature. This appendix is essential reading for a full understanding of some results to be discussed in this section.

Figure 3 represents the numerical case study. The whole set of parameters defining the excavation, the ground and the retaining structure was conceived in order to provide, under certain circumstances, a situation of failure by loss of vertical equilibrium.

The excavation, 20m wide and 18m deep, is supported by a 0.4m thick concrete soldier-pile wall with five anchor levels inclined 45°. The ground consists of a homogeneous clay deposit 18m thick (with constant undrained shear strength, c_u, of 80kPa) underlain by a very stiff material. The horizontal components of anchor prestressing forces are equivalent to a trapezoidal diagram with a maximum pressure of $0.3\gamma H$. The steel soldier-piles are HEB 120 (S235), with an average horizontal spacing of 1m.

Figure 3 includes further details concerning the parameters of the soil, of the retaining structure and of the finite element mesh, which is represented for the final construction stage. Both soil and wall were modeled with 8-node isoparametric quadrilateral elements; 6-node joint elements were used for the soil-to-wall interface; the anchors and the soldier-piles were simulated by 2-node bar elements. The nodes at the bonded length of both anchors and soldier-piles are fixed points, located at the firm ground underneath the excavated soil. Both the soil and the the soil-to-wall interface were analyzed in total stresses with an elastic perfectly plastic behavior, using Tresca yield surface. Bearing in mind that the fundamental issue is to study situations in which soil mass and the retaining structure are on the verge of failure, the use of such simple constitutive mode should not affect the main conclusions of the paper.

The excavation was simulated according to the construction sequence detailed in Table 2, and partially described in Figure 3 and in Appendix I.

Three analyses - A, B and C - were performed, covering variations of the structural resistance of the soldier-piles and of the resistance of the soil-to-wall interface, according to Table 3.

The soldier-piles are assumed as linear elastic in analysis A and as elastic perfectly-plastic in analyses B and C. With regard to the yielding axial load on the piles, two situations have to be considered (see Figure 1 and Appendix I for better understanding): i) in the excavation stages, since a given length of the soldier-piles becomes unconfined, it coincides with the buckling load; ii) in the stages corresponding to the construction of concrete panels or to anchor prestressing,

since soldier-piles are confined by the soil, that load is given by the product of the yielding stress of the steel by the cross sectional area of the pile.

The finite element analyses were carried out using a mixed incremental and iterative procedure with a constant stiffness approach at each increment and the residual force convergence criterion. The specified tolerance was 0.1%, for a maximum number of iterations equal to 20000.

3.2 Influence of the resistance of the soldier-piles (analysis A versus analysis B)

3.2.1 Introduction

A detailed discussion of the results from analyses A and B is now presented.

If anchor loads after prestressing were constant and a complete mobilization was achieved of upward shear stresses at the soil-to-wall interface, vertical equilibrium (expressed by equation 1) would not be verified beyond stage 15 for analysis B. As discussed below, the results are rather curious: plastification of the soldier-piles occurs sooner (stage 13) but collapse is achieved much later (stage 19).

In numerical terms, collapse means lack of convergence of the analysis. Table 4 summarizes the evolution of the norm of the residual force vector, expressed as a percentage of the external forces, r, and of the displacement of the top of the wall with the number of iterations for stage 19 of analysis B. Bearing this fact in mind, the results presented below for stage 19 of analysis B should be regarded with reticence, although they give useful indications regarding the evolution of the field variables under analysis.

3.2.2 Loads on soldier-piles

Figure 4 presents the evolution of the load acting on the soldier-piles in analyses A and B.

For analysis A, the load increases as construction proceeds with more significant increments at the anchor prestressing stages (stages 6, 9, 12, 15 and 18). Note that there is no limitation of the pile load in analysis A. The increments in the excavation stages are due to the loss of vertical support from the soil at the base of the concrete panels and because the soil moves downward relatively to the wall.

Analysis B provides identical results to analysis A until stage 12. At this stage, since the piles are still confined by the soil, the mobilized resistance exceeds the buckling resistance. Yielding

by buckling takes place at the following stage, corresponding to excavation level 4.

3.2.3 Shear stresses at the soil-to-wall interface

Figure 5 presents the shear stress applied by the soil to the back wall face for stages 10 to 19 for analyses A and B (positive values correspond to upward stress). The peaks on the graphs close to the base of each excavation level are just the effect of horizontal joint elements at the base of the wall panels (see Appendix I). Up to stage 12, the results of both analyses coincide.

Due to plastification by buckling of the soldier-piles in stage 13 of analysis B, the results become discrepant, with a significant increase in the upward (positive) stresses in this analysis, in the stage immediately following plastification. In contrast, analysis A reveals a clear trend to downward (negative) shear stresses being mobilized with the progress of the construction.

An alternative way of analyzing the soil-wall interaction by shear is through the integration of the shear stresses along the interface, for each construction stage. This can be observed in Figure 6, for both analyses, where the total shear force is expressed as a percentage of the resistant force of the interface. Positive values correspond to upward forces applied to the wall.

The evolution of the mobilized resistance at the soil-to-wall interface can be described as follows. Up to stage 7 there is a considerable mobilization of the upward resistance. This derives from the elastic heave induced in the ground by the early excavations stages (see, for instance, Figure 7(a)) and from anchor prestressing. This trend is reversed due to the increase in horizontal movements of the wall and the consequent settlements of the supported ground. In analysis A this reversion proceeds until the end of construction, with the final shear force applied by the soil to the wall being downwards. This is a typical situation in embedded retaining walls with sound foundation conditions (Matos Fernandes et al., 1993).

For analysis B, on the other hand, after pile plastification at stage 13, a different trend can be observed: the settlement of the wall induces a strong increase in upward stresses. Collapse is reached at stage 19, and the mobilized resistance sharply diminishes, apparently towards zero. This small mobilization of the interface resistance can also be seen in the previously mentioned small-scale tests performed by Plant (1972).

3.2.4 Soil displacements

Figure 7 shows the displacements of the face of the cut and of ground surface provided by analyses A and B for excavation levels 1 to 6 (stages 4, 7, 10, 13, 16 and 19).

As could be expected, at the early excavation levels (levels 1 to 3) the results from both analyses coincide (Figure 7(a)): the horizontal and vertical displacements are modest and exhibit a smooth increase with the progress of the excavation. This pattern fully applies to analysis A up to the completion of the construction, as illustrated by Figure 7(b) (note the change in the scale of displacements). On the contrary, results from analysis B (Figure 7(c)) reveal very large movements, both vertical and horizontal, beyond stage 13 (excavation level 4) due to pile yielding, leading to the collapse of the system at stage 19. That correlation between vertical and horizontal displacements was pointed out by Briaud and Kim (1998). The convex shape of the ground surface in the late construction stages for analysis B shows that the wall settles in relation to the adjacent soil.

3.2.5 Evolution of anchor forces

Since the resistance of soldier-piles is fully mobilized beyond stage 13 in analysis B and the shear force at the soil-to-wall interface could not significantly change after pile plastification, the rise in the total vertical resistant force (right-hand side of equation 1) must be moderate in the subsequent construction stages. So, when the vertical applied load increases (left-hand side of equation 1), the resistant force could not be mobilized in the same amount, and consequently the anchor forces must be reduced. Figure 8 illustrates the evolution of anchor loads in both analyses A and B, expressed as a percentage of the lock-off force.

Anchor load variations in analysis A are small, usually in the range of $\pm 8\%$. The same variations occur for analysis B until pile plastification. After that, an important decrease in anchor load is observed, reaching about 30% in anchor level 3 at stage 16 and 100% in anchor levels 1, 2 and 3 at stage 19. Level 5, however, exhibits a significant increase, which is consistent with the collapse movement of the wall, as Figure 7(c) shows. These results concerning anchor load evolution at collapse fully agree with those previously mentioned from small-scale tests.

3.2.6 Analysis of the vertical equilibrium

The evolution of the total vertical load on the wall (anchor forces plus wall weight) together with the shear force at the interface and the reaction mobilized on the soldier-piles are presented in Figure 9, for both analyses A and B.

For analysis A it is clear that the vertical load is essentially carried by the soldier-piles. In fact, at the end of construction, the reaction on the soldier-piles is even greater than the total vertical load on the wall, since the shear force at the interface is directed downwards.

In analysis B, the following comments apply:

- the vertical load is lower than in analysis A due to the progressive decrease of the anchor forces;
- after buckling of the soldier-piles (stage 13), a progressive increase of the shear force at the interface can be observed until stage 18, reaching values of the same order of magnitude of the one carried by the piles.

3.3 Influence of the resistance of the soil-to-wall interface (analysis B versus analysis C)

The discussion of the results from analysis B showed that the collapse of the system can occur without a complete mobilization of the interface resistance. Nevertheless, it could be argued that if the excavation had stopped at stage 16 (15m deep) vertical stability would have been ensured with the significant contribution from the upwards shear force at the interface.

To find out whether the resistance of the interface is relevant for vertical stability, a third analysis (analysis C) was undertaken: with the exception of the soil-to-wall resistance, which has been considered as null, all the other data coincide with analysis B.

Figure 10 presents the displacements obtained from analyses B and C until stage 16/5th excavation level (collapse takes place for both analyses at the last excavation level). It is rather interesting to note that the performance of analysis C, as far as movements are concerned, is not worse (it could even be said that it is better) than analysis B.

In order to clarify these apparently strange results, the whole set of forces applied to the wall at stage 16 was computed, as shown in Figure 11. Note that the reaction of the soldier-piles is the same in both analyses (it corresponds to the buckling load) as well as the wall weight. Since

the shear force at the interface in analysis C is null, in this analysis the vertical anchor force must be smaller, and the same applies to the horizontal anchor force.

It can then be seen that the larger horizontal anchor force applied to the soil in analysis B does not lead to lower displacements. This arises from the vertical force applied by the wall to the ground, through the interface, which is responsible for an increase on the horizontal force required for stability. A very interesting situation is then observed: two analyses with distinct soil-structure interactions, involving quite discrepant forces but leading to comparable displacements.

These results indicate that further clarification is required for the role of the soil-to-wall interface resistance in the vertical equilibrium of the soldier-pile walls. A reassessment of the problem is proposed in the next section by an alternative approach.

4 APPROACH BASED ON LIMIT ANALYSIS

4.1 Formulation of the problem

For ensuring stability of a cut in a soil mass the retaining wall has to provide sufficient horizontal force. If there is adhesion at the soil-to-wall interface, the mobilized value influences the horizontal force needed to stabilize the cut. In permanent soldier-pile walls, this horizontal force is only controlled by the anchors.

The previous comments on the finite element calculations make clear that if pile resistance is less than a given value, anchor forces will decrease, with the corresponding horizontal force being insufficient to ensure equilibrium of the supported ground.

An upper bound solution can be performed to determine the horizontal force value required to prevent excavation collapse. To that end the kinematically compatible plastic deformation field suggested by Figure 12 will be considered. This consists in assuming plastic deformations concentrated on a plane surface intersecting the excavation toe and defined by angle α. Thus the upper soil block moves relatively to the remaining soil by a value δ, in the direction of the sliding surface. The work of external forces should then be equal to the work of plastic deformation, leading to:

$$(W_s + pc_a H_w)\,\delta sin\alpha - A_{lim} cos\beta \delta cos\alpha = \frac{c_u H}{sin\alpha}\delta \tag{3}$$

where A_{lim} is the total anchor force at the limit state, W_s is the weight of the soil wedge and

the other symbols have the meaning previously described.

If μ is defined as

$$\mu = \frac{1}{2}\gamma H^2 \tag{4}$$

γ being the soil unit weight, and if the stability number, N_s, is

$$N_s = \frac{\gamma H}{c_u} \tag{5}$$

equation (3) can be rewritten as follows:

$$1 - \frac{A_{lim} cos\beta}{\mu} + \left(\frac{1}{2}\chi_{am} tan\alpha - \frac{1}{sin2\alpha}\right)\frac{4}{N_s} = 0 \tag{6}$$

where

$$\chi_{am} = \frac{p c_a H_w}{c_u H} \tag{7}$$

represents a normalized mobilized resistance. The value of α maximizing A_{lim} can be obtained by:

$$\frac{dA_{lim}}{d\alpha} = 0 \Rightarrow tan\alpha = (1 - \chi_{am})^{-1/2} \tag{8}$$

Using equation (8) in (6) leads to:

$$1 - \frac{A_{lim} cos\beta}{\mu} - (1 - \chi_{am})^{1/2}\frac{4}{N_s} = 0 \tag{9}$$

For a self supported excavation, $p = 0$, $A = 0$, and N_s assumes its critical value, which is equal to

$$N_s = N_{scrit} = 4 \tag{10}$$

Therefore, an excavation is self supported if the stability number, N_s, is less than or equal to the critical stability number, N_{scrit}. Since the previous derivation is based on an upper bound solution, the value of $N_{scrit} = 4$ is unsafe. In fact, the self supported cut problem has been extensively studied by limit analysis methodologies and the more precise values are known (Pastor et al., 2000): i) $N_{scrit} = 3.7603$, based on a lower bound solution (safe); ii) $N_{scrit} = 3.7859$, based on an upper bound solution (unsafe).

As it was shown that "4" in equation (9) is the critical stability number and bearing in mind

that value gives unsafe results and is quite far from the (unknown) exact value, it is proposed to replace "4" by N_{scrit} in that equation and to perform computational tests in order to evaluate a proper value for N_{scrit}. The following semi-empirical equation is then proposed by adapting equation (10) according to the previous considerations:

$$1 - \frac{A_{lim} cos\beta}{\mu} - (1 - \chi_{am})^{1/2} \frac{N_{scrit}}{N_s} = 0 \tag{11}$$

By replacing the value of A from equation (1) in equation (11) the following equation is obtained:

$$N_{pile}^{lim} - W_w = \mu tan\beta \left\{ 1 - \left[\frac{2\chi_{am}}{N_{scrit} tan\beta} + (1 - \chi_{am})^{1/2} \right] \frac{N_{scrit}}{N_s} \right\} \tag{12}$$

For a given soil-to-wall interface resistance, c_a, and a given soil resistance, c_u, this equation gives an estimate of the minimum pile resistance value leading to a limit state. The value depends on the ratio, p, of interface resistance mobilization in the limit state situation, which is not known beforehand.

For the structure with the geometrical and mechanical characteristics considered in this paper ($N_s = 4.5$ and $\beta = 45^o$) and for the range of N_{scrit} of 3.75 to 3.85, the minimum values of pile resistance, $N_{pile}^{lim} - W_w$, have been determined using equation (12), as a function of the normalized mobilized resistance, χ_{am}. The results represented in Figure 13 show that mobilization of higher percentages of resistance could be detrimental, in the sense that stronger piles would be required. There is a certain critical value of χ_{am} for which the pile resistance needed to ensure equilibrium is minimum. For $\beta = 45^o$ this critical value of χ_{am} is positive and close to null.

The analysis of Figure 13 highlights two important features of the finite element results previously presented:

- the fact that collapse occurs without full mobilization of the soil-to wall interface resistance in analysis B;
- the quite similar performance with regard to displacements obtained from analyses B and C.

The results of Figure 13 will be compared, in the following section, with finite element results.

4.2 Comparison with the finite element results

The finite element program used in section 3 may be employed to evaluate the critical stability number. In fact, by performing successive calculations in which the pile resistance is changed while all the other parameters are kept constant, it is possible to find, with a relatively small error, the pile resistance value for which the excavation collapses. In order to define this value, both the analysis of the evolution of displacements and the lack of convergence of the calculation have been considered.

This methodology was applied to the previously presented case study considering different values of soil-to-wall resistance. Figure 14 illustrates the total displacements of the upper point of the cut face as a function of the resistance of the piles from four sets of calculations.

For all situations the value of the minimum pile resistance ensuring soil stability is almost the same. This means that, when limit state is reached, the mobilized resistance should be the same, regardless of the value of the soil-to-wall interface resistance. In fact, the calculated mobilized interface resistance is very similar in all cases and is close to null. This result could somehow be predicted bearing in mind the shape of the curves relating $N_{pile}^{lim} - W_w$ with χ_{am} in Figure 13, which indicates that the minimum value of the pile resistance is associated with a very low interface resistance mobilization. In Figure 13 the finite element results are also represented and show a good agreement with the previously referred curves. It should be noted that the results obtained with c_a of 10, 30 and 50kPa are represented by the same point.

Figure 14 allows to conclude that the minimum value of $N_{pile}^{lim} - W_w$, which is compatible with the stability of the supported soil is about 465kN/m. Since the wall weight is 150kN/m, the value of pile resistance required to prevent collapse is 615kN/m. In analysis B, this resistance has been assumed as equal to 605kN/m, which means that the collapse of the excavation was to be expected.

The calculation results commented above correspond to a soil that is underlain by a very hard ground (see Figure 3), which means that, in Figure 12, the depth of the rigid layer, H_r coincides with the depth of the excavation ($H_r = H = 18\,\mathrm{m}$). Since this can affect the value of N_{scrit}, an additional set of calculations has been performed considering $H_r = 25\,\mathrm{m}$. The influence of this parameter was confirmed, as Figure 14 also shows, although it doesn't seem to be determinant.

4.3 Generalization

The study presented in the previous section for determining N_{scrit} has been carried out considering $N_s = 4.5$ and $\beta = 45^o$. Other values of N_s and β can, however, be considered.

Figure 15 summarizes the results of the application of equation (12) for other values of β, with $N_s = 4.5$. For each value of β, two lines are drawn, corresponding to $N_{scrit} = 3.75$ and 3.85.

The figure illustrates the complexity of the soil-structure interaction in this type of retaining wall, which is highly affected by anchor inclination. In fact, both the favorable and unfavorable effect of the normalized mobilized resistance depend on β. The increase (upwards or downwards, according to the value of β) in the mobilized resistance is favorable (leading to a lower pile resistance corresponding to the limit state) until a certain value of χ_{am} is reached.

The problem can be summarized as follows: analyzing the right part of Figure 12, it can be seen that an increase of χ_{am}, implying greater downward tangential forces applied to the supported ground, produces an adverse effect on the stability of the soil mass; on the other hand, an increase in $Acos\beta$ is advantageous to the stability. But an increase on χ_{am} can only be accompanied by an increase in $Acos\beta$. Then, the global effect is favorable or unfavorable depending on the value of χ_{am} and on the anchor inclination. A favorable effect corresponds, of course, to lower values of $N_{pile}^{lim} - W_w$ whereas an unfavorable effect implies greater values of $N_{pile}^{lim} - W_w$. The relationship between χ_{am}, β and $N_{pile}^{lim} - W_w$ is shown in Figure 15.

Figure 16 presents the influence of N_s on N_{pile}^{lim} for a constant value of $\beta = 45^o$ and for N_{scrit} of 3.75 and 3.85, by applying equation (12). The expected result is obtained, namely, less resistant soils (higher N_s) demand more resistant piles. A few more finite element results are presented in the same figure, revealing a relatively good agreement with the theoretical curves derived from that equation. For high values of N_s (not shown in the figure), where base stability problems start to be involved, the analytical results are no longer confirmed by finite element calculations. However, such conditions are beyond the scope of this paper, since soldier-pile walls are typically applied to excavations with low to moderate stability numbers.

5 CONCLUSIONS

The numerical results obtained in this study corroborate and clarify the evidences from incidents and failures in excavation works supported by anchored soldier-pile walls, which have been reported in the literature. The pattern of the failure mechanism by loss of vertical equilibrium is, to a great extent, common to the one of embedded conventional walls: large or very large vertical and horizontal displacements of the ground and of the wall, inducing a progressive unloading of the anchors, thereby leading to the collapse of the system. The main specific point of this failure mechanism in soldier-pile walls is that it is triggered by the failure of the soldier-piles. This can occur by buckling of the piles themselves (therefore, a structural failure) or by insufficient bearing capacity of their foundation.

The soil-to-wall interaction by shear at the back wall face is a critical factor in understanding vertical equilibrium. In simple terms, if the vertical resistance of the soldier-piles is high, downward shear stresses transmitted to the wall by the supported ground will increase with the progress of construction, together with small vertical and horizontal displacements and modest variations in anchor loads. This corresponds to a good performance of the retaining structure.

Conversely, pile yielding (by buckling or by bearing capacity failure) will induce wall settlements, leading to the mobilization of upward shear stresses at the back wall face. But such settlements also induce unloading of the anchors and, then, lateral wall displacements and lateral and vertical displacements of the supported ground. However, it was particularly interesting to observe that when soil-to-wall interface resistance is considered null, the performance of the excavation is not worse.

This apparent contradiction has been clarified by a re-assessment of the vertical equilibrium issue using limit analysis, based on upper bound solutions. It has been shown that the minimum resistance of the vertical piles required to ensure stability can be evaluated as a function of the stability number of the excavation, anchor inclination and the critical stability number, N_{scrit}. Finite element results were used to estimate this number.

This re-assessment allowed to highlight the complexity of the soil-structure interaction in this type of retaining wall, which is highly dependent on anchor inclination.

As a general conclusion, it can be said that lateral upward resistance should not be considered in the design of soldier-pile retaining structures and similar walls. In fact, for N_s near the maximum acceptable value for the type of retaining walls under study, even a partial mobi-

lization of such resistance seems to involve displacements and anchor load drops which lead to unsatisfactory support performance. The piles should therefore be designed to support at least the total vertical load imposed by the anchor forces and by the wall weight.

Design based on the theoretical equation of the minimum pile resistance presented in the paper is not suitable unless very high safety factors are considered, because this is based on a limit situation that involved pile plastification, which for design purposes should of course be avoided.

ACKNOWLEDGMENTS

The authors would like to express their appreciation for the valuable contributions to this paper of Dr. Jorge Almeida e Sousa, from University of Coimbra, and of Dr. J. Couto Marques, from University of Oporto.

APPENDIX I.

The modeled construction sequence is schematically represented in Figure 17 and consists of the following steps (Guerra et al., 2001):

- stage 0 corresponds to the application of the initial stress state;
- in stage 1, vertical piles are put in place and the excavation for the installation of the top concrete beam of the wall is performed; at this stage, the elements used to model the piles are completely independent from the other elements of the mesh and no effect of their installation is considered; the toe of the soldier piles is fixed; horizontal joint elements are placed at the base of the beam;
- in stage 2, the loads due to the weight of the concrete beam are applied on the horizontal joint elements;
- stage 3 corresponds to the placement of the elements representing the concrete beam and of the vertical joint elements to model the soil-to-wall interface; it should be noted that if concrete elements were placed at the same time as their weight, part of the resistance at the soil-to-wall interface would be unrealistically mobilized; also in stage 3, a small vertical

bar element with high stiffness is activated, connecting the steel piles to the concrete wall; in fact, this bar element has no effect (it will be removed in the next stage) because at this level there is no anchor, but, for simplicity, the procedure used is the same as for stage 6, which includes an anchor load and in which it will be used;

- in stage 4, the first excavation level is completed, the horizontal joint elements are removed and new horizontal joint elements are put in place; at this same stage the small bar as well as the top bar of the initial steel pile are removed and replaced by a bar with a limit load corresponding to the buckling load of the soldier-pile; the previous limit load of the pile was higher than the buckling load because until this stage the pile had been confined by the soil;

- in stage 5, loads due to the weight of the first concrete panel are applied, in a similar way as presented in stage 2;

- in stage 6, both concrete elements and the vertical joint elements are activated; the bar placed in stage 4 is removed, and a small bar with high stiffness is placed, connecting the concrete elements to the soldier-pile; the load due to the first anchor level is applied;

- in stage 7, the construction process is similar to the one of stage 4 with a further operation being simulated, which consists of the activation of the bar element corresponding to the first anchor level;

- in stage 8, the construction process is similar to the one of stage 5; further sets of construction stages similar to the previous ones are then performed until the end of construction.

APPENDIX II. NOTATION

The following symbols are used in this paper:

A anchor force per unit length of the wall;

A_h horizontal component of anchor force per unit length of the wall;

A_v vertical component of anchor force per unit length of the wall;

A_{lim} anchor force at the limit state per unit length of the wall;

c_a interface resistance (adhesion);

c_u soil undrained shear strength;

d total displacement;

$E_{anchors}$ Young modulus of anchor cables;

E_{piles} Young modulus of soldier-piles;

E_{wall} Young modulus of the wall;

E_u soil undrained Young modulus;

F_l shear force mobilized at the soil-to-wall interface per unit length of the wall;

H excavation depth;

H_w wall height;

H_r depth of rigid layer;

K_0 initial horizontal stress coefficient;

K_t shear stiffness of the interface;

L_p height of the concrete wall panel;

N_{pile} vertical reaction mobilized on the soldier-piles per unit length of the wall;

N_{pile}^{lim} limit value of pile load per unit length of the wall;

N_s stability number of the excavation;

N_{scrit} critical stability number of the excavation;

p ratio of mobilization of the interface resistance;

r norm of the residual force vector in percentage of the external forces;

R_n normal force at the soil wedge sliding surface per unit length of the wall;

R_t shear force at the soil wedge sliding surface per unit length of the wall;

$S_{anchors}$ cross sectional area of anchor cable per unit length of the wall;

S_{piles} cross sectional area of soldier-piles per unit length of the wall;

W_s weight of the soil wedge per unit length of the wall;

W_w wall weight per unit length;

α inclination of the sliding surface limiting the soil wedge;

β anchor inclination angle with the horizontal plan;

χ_{am} normalized mobilized resistance;

δ displacement of the soil wedge in the direction of the sliding surface;

γ unit weight of soil;

μ auxiliary symbol, equal to $0.5\gamma H^2$;

ν_u Poisson coefficient of soil in undrained conditions.

APPENDIX III. REFERENCES

Almeida e Sousa, J. (1998). "Tunnelling in soft ground. Behavior and numerical simulation". PhD thesis, Faculdade de Ciências e Tecnologia, University of Coimbra, Coimbra, Portugal (in Portuguese).

Barley, A. D. (1997). Contribution for discussion of session no 5. *Ground anchorages and anchored structures, Proceedings of the international conference organized by the Institution of Civil Engineers*, 592–596, London. Thomas Telford.

Briaud, J.-L. and Kim, N.-K. (1998). Beam-column method for tieback walls. *ASCE Journal of Geotechnical and Geoenvironmental Engineering Division*, 124(1),67–79.

Broms, B. B. and Stille, H. (1976). "Failure of anchored sheet pile walls". *J. Geotech. Engrg. Div.*, ASCE, 102(3),235–251.

Cacoilo, D., Tamaro, G., and Edinger, P. (1998). "Design and performance of a tied-back sheet pile wall in soft clay". *Design and Construction of Earth Retaining Systems, Geotechnical Special Publication No 83*, ASCE,14–25.

Cardoso, A. J. M. S. (1987). "Soil nailing applied to excavations". PhD thesis, Faculdade de Engenharia, University of Oporto, Oporto, Portugal (in Portuguese).

ENV 1993-1.1 (1992). Eurocode 3, Design of steel structures, Part 1.1, General rules and rules for buildings. CEN, European Committee for Standardization, Brussels.

Gould, J. P., Tamaro, G. J., and Powers, J. P. (1992). "Excavation and support systems in urban settings". *Excavation and Support for the Urban Infrastructure, Geotechnical Special Publication No 33*, ASCE,144–171.

Guerra, N. M. C. (1999). "Collapse mechanism of Berlin-type retaining walls by loss of vertical equilibrium". PhD thesis, Instituto Superior Técnico, Technical University of Lisbon, Lisbon, Portugal (in Portuguese).

Guerra, N. M. C., Gomes Correia, A., Matos Fernandes, M., and Cardoso, A. S. (2001). "Modelling the collapse of Berlin-type walls by loss of vertical equilibrium: a few preliminary results". *3rd International Workshop Applications of Computational Mechanics in Geotechnical Engineering*, 231–238, Oporto, Portugal.

Hanna, T. H. (1968). "Design and behavior of tied-back retaining walls". *Proc. 3rd Budapest Conf. Soil Mech. Found. Eng*, 410–418, Budapest, Hungary.

Hanna, T. H. and Abu-Taleb, M. G. A. (1972). "Anchor supported walls: research and practice". *Ground Engrg.*, London, 5(2),16–20.

Hanna, T. H. and Matallana, G. A. (1970). "The behavior of tied-back retaining walls". *Can. Geotech. J.*, Ottawa, Canada, 7(4),372–396.

Matos Fernandes, M. A., Cardoso, A. J. S., Trigo, J. F. C., and Marques, J. M. M. C. (1993). "Bearing capacity failure of tied-back walls: a complex case of soil-wall interaction". *Computers and Geotechnics*, 15,87–103.

McRostie, G. C., Burn, K. N., and Mitchell, R. J. (1972). "The performance of tied-back sheet piling in clay". *Can. Geotech. J.*, Ottawa, Canada, 9,206–218.

Pastor, J., Thai, T. H., and Francescato, P. (2000). "New bounds for the height limit of a vertical slope". *International Journal for Numerical and Analytical Methods in Geomechanics*, 24,165–182.

Plant, G. W. (1972). "Anchors inclination - its effects on the performance of a laboratory scale tied-back retaining wall". *Proc. Instn. of Civ. Engrs.*, London, 53, part 2,257–274.

Shannon, W. L. and Strazer, R. J. (1970). "Tied-back excavation wall for Seattle First National Bank". *Civ. Engng.*, ASCE, 40,62–64.

Slater, W. M. (1967). "Prestressed anchors and tie-backs in greater use". *Daily Commercial News and Building Record*, 16–17. Paper referred by Hanna (1968).

Stocker, M. F. (1991). "Contribution for discussion n. 4b". *Proceedings of 10th European Conference of Soil Mechanics and Foundation Engineering*, vol. 4, 1368, Firenze, Italy.

Ulrich, E. J. J. (1989). "Tieback supported cuts in overconsolidated soils". *J. Geotech. Engrg.*, ASCE, 115(4),521–545.

Ware, K. R., Mirsky, M., and Leuniz, W. E. (1973). "Tieback wall construction - results and controls". *J. Soil Mech. and Found. Div.*, ASCE, 99(12),1135–1152.

White, R. E. (1974). "Anchored walls adjacent to vertical rock cuts". *Proceedings Conference on Diaphragm Walls*, 35–42, London, U.K. Institution of Civil Engineers.

Winter, D. G. (1990). "Pacific First Center performance of the tieback shoring wall". *Design and Performance of Earth Retaining Structures, Geotechnical Special Publication No 25*, ASCE,764–777.

Table 1: Incidents and accidents of tied-back walls related with poor vertical support

Reference (1)	Retaining wall (2)	Location, date (3)	Behavior (4)
Slater (1967); Hanna (1968)	soldier-pile, temporary	N.A., N.A.	very large horizontal and vertical (90cm) wall displacements
Shannon and Strazer (1970)	soldier-pile, temporary	Seattle, USA, N.A.	large vertical wall displacements (7.6cm)
McRostie et al. (1972)	sheet-pile	Ottawa, Canada, 1970	high anchor load drops; possibility of vertical movement of the wall
Ware et al. (1973)	soldier-pile, temporary	Washington, USA, 1973	piles settled due to downdrag from tie-backs (5.1cm)
White (1974)	sheet-pile	Pittsburgh, USA, 1968	excavation below wall toe; wall settlement of 0.15m
White (1974)	soldier-pile	Washington, USA, 1971	excavation below wall toe; vertical failure; wall settlement of 0.60m
Broms and Stille (1976)	sheet-pile	Norrköping, Sweden, 1969	wall settlement (5-10cm) and lateral displacement caused by pore pressures due to driving of piles
Broms and Stille (1976)	sheet-pile	Västerås, Sweden, 1972	lateral wall displacement (5-15cm); large settlement of supported soil; increase in anchor load force
Broms and Stille (1976)	sheet-pile	Gothenburg, Sweden, 1974	lateral wall displacement (51-61cm); settlement of supported soil (41cm)
Broms and Stille (1976)	sheet-pile	Stockholm, Sweden, N.A.	large lateral and vertical displacements; drop in anchor load
Ulrich (1989)	concrete pile wall	Huston, USA, 1973	very large wall settlements compared with the horizontal displacements
Winter (1990)	soldier-pile, temporary	Seattle, USA, 1988	large settlements of supported soil (6cm); possibility of vertical settlement of the wall
Stocker (1991)	concrete pile wall	N.A., N.A.	sudden pile settlement (15cm)
Gould et al. (1992)	soldier-pile, temporary	Washington, USA, 1972	excavation below wall toe; vertical failure due to exposure of slip planes in the rock bearing layer
Barley (1997)	sheet-pile	N.A., N.A.	excavation below wall toe; vertical failure
Cacoilo et al. (1998)	sheet-pile	Boston, USA, N.A.	large horizontal displacements but no significant anchor load changes; possibility of wall settlement
Guerra (1999)	soldier-pile, permanent	Oporto, Portugal, 1990-91	significant horizontal and vertical wall displacements, loss of anchor forces; some damage in the vicinity
Guerra (1999)	soldier-pile, permanent	Oporto, Portugal, 1992-93	buckling of soldier-piles; large horizontal and vertical wall displacements; surface settlements up to 20cm
Guerra (1999)	soldier-pile, permanent	Lisbon, Portugal, 1993	wall collapse by vertical instability
Guerra (1999)	soldier-pile, permanent	Gaia, Portugal, 1994-95	buckling of soldier-piles; significant horizontal and vertical wall displacements

N.A.: not available.

Table 2: Construction sequence adopted in the numerical case study.

Level	Depth	Construction Stage		
	(m)	Excavation	Panels (weight)	Panels (stiffness)+anchor pre-stress
(1)	(2)	(3)	(4)	(5)
Top beam	0.8	1	2	3 (no anchor)
1st level	3.0	4	5	6
2nd level	6.0	7	8	9
3rd level	9.0	10	11	12
4th level	12.0	13	14	15
5th level	15.0	16	17	18
6th level	18.0	19	–	–

Table 3: Limit pile loads and soil-to-wall interface resistance in analyses A and B

Analysis	Limit Pile Loads (kN/m)		Soil-to-wall interface resistance (adhesion) (kPa)
	Unconfined (buckling resistance)	Confined (axial plastic resistance)	
(1)	(2)	(3)	(4)
A	∞	∞	50
B	605	847	50
C	605	847	0

Note: Unconfined limit pile load is the buckling resistance determined using Eurocode 3 (ENV 1993-1.1, 1992); confined limit pile load is the limit pile load when pile is confined by the soil; it was consider equal to the axial plastic resistance. Both confined and unconfined resistance were determined using the average value of the steel yield stress (249MPa for steel S235) instead of the characteristic one.

Table 4: Norm of the residual force vector in percentage of the norm of the external force vector (r) and displacements of the top of the wall (d) for stage 19 of analysis B.

Iterations	r	d
	(%)	(m)
(1)	(2)	(3)
10	5.83	0.151
100	2.00	0.246
1000	0.77	0.581
2000	0.55	0.783
10000	0.24	1.601
20000	0.21	2.401

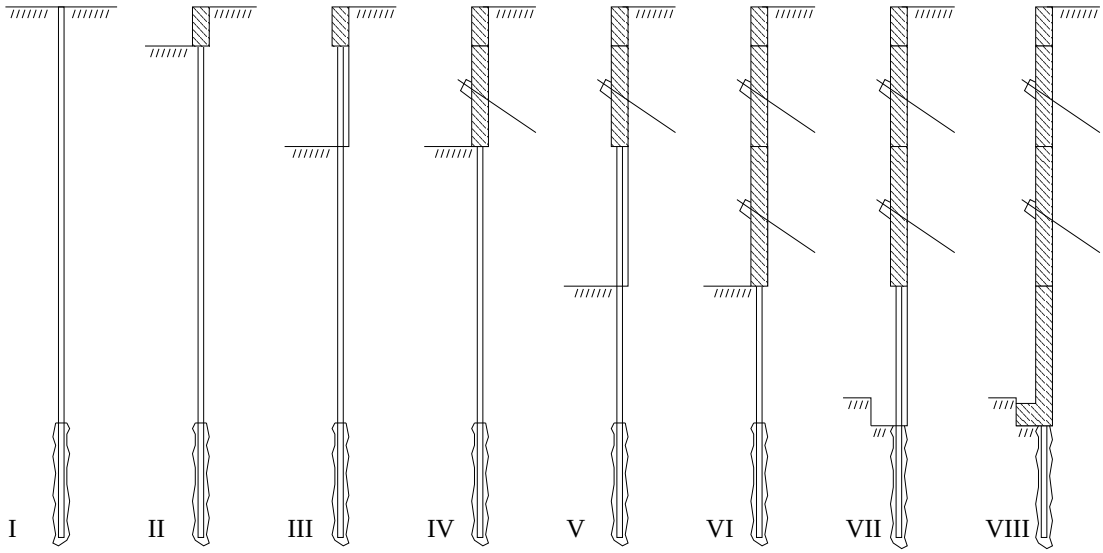

Figure 1:

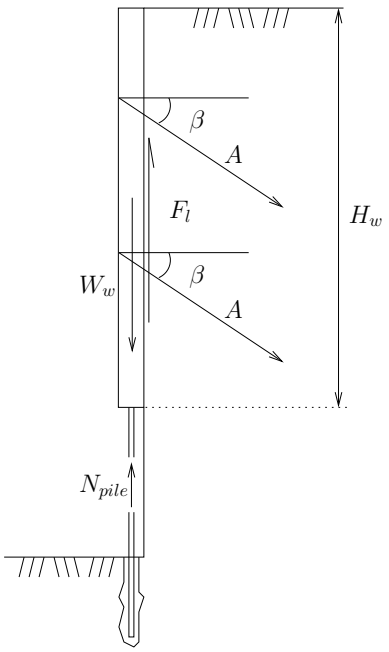

Figure 2:

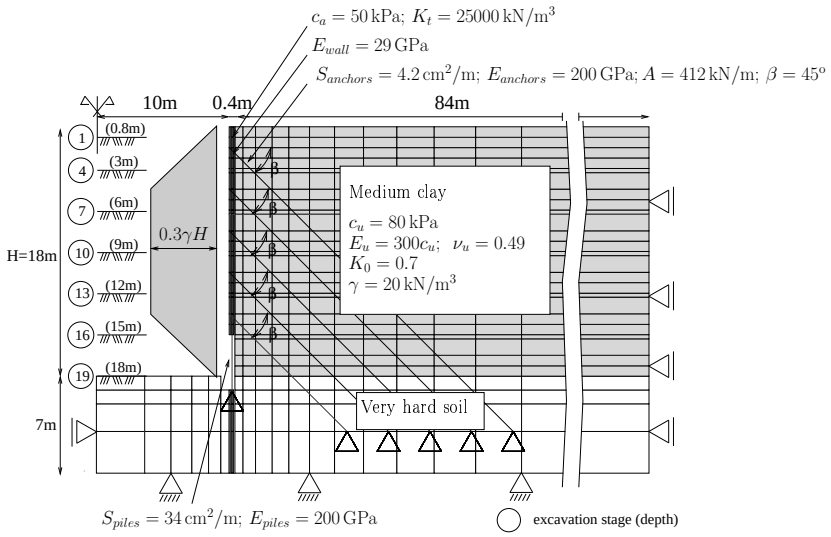
$c_a = 50\,\mathrm{kPa};\ K_t = 25000\,\mathrm{kN/m^3}$
$E_{wall} = 29\,\mathrm{GPa}$
$S_{anchors} = 4.2\,\mathrm{cm^2/m};\ E_{anchors} = 200\,\mathrm{GPa};\ A = 412\,\mathrm{kN/m};\ \beta = 45^o$
10m
0.4m
84m
(0.8m)
(3m)
(6m)
(9m)
(12m)
(15m)
(18m)
H=18m
7m
$0.3\gamma H$
Medium clay
$c_u = 80\,\mathrm{kPa}$
$E_u = 300c_u;\ \ \nu_u = 0.49$
$K_0 = 0.7$
$\gamma = 20\,\mathrm{kN/m^3}$
Very hard soil
$S_{piles} = 34\,\mathrm{cm^2/m};\ E_{piles} = 200\,\mathrm{GPa}$
excavation stage (depth)

Figure 3:

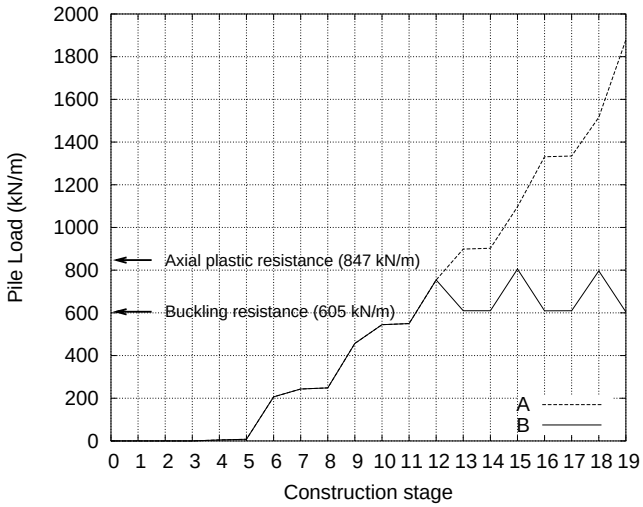
Pile Load (kN/m)
Construction stage
Axial plastic resistance (847 kN/m)
Buckling resistance (605 kN/m)
A
B
0
200
400
600
800
1000
1200
1400
1600
1800
2000
0 1 2 3 4 5 6 7 8 9 10 11 12 13 14 15 16 17 18 19

Figure 4:

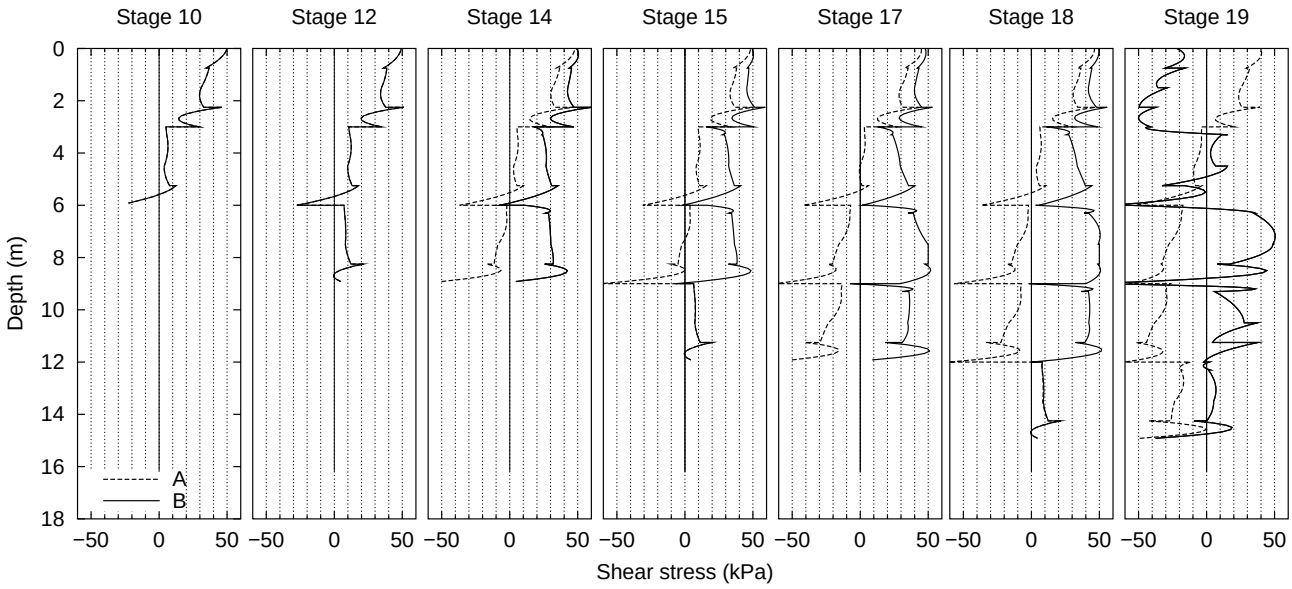
Stage 10
Stage 12
Stage 14
Stage 15
Stage 17
Stage 18
Stage 19
Depth (m)
0
2
4
6
8
10
12
14
16
18
A
B
−50
0
50
Shear stress (kPa)

Figure 5:

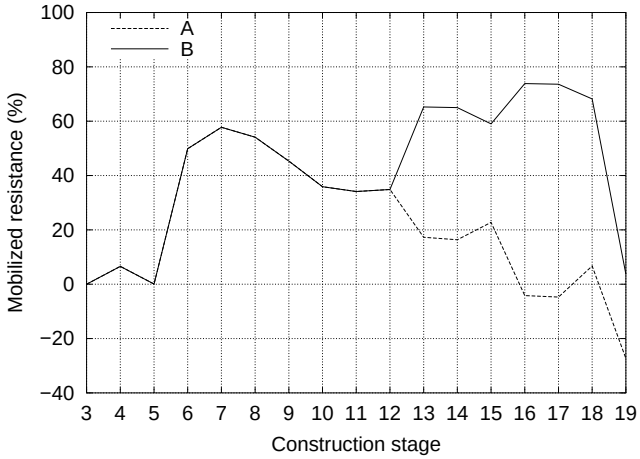
A
B
Mobilized resistance (%)
100
80
60
40
20
0
−20
−40
3 4 5 6 7 8 9 10 11 12 13 14 15 16 17 18 19
Construction stage

Figure 6:

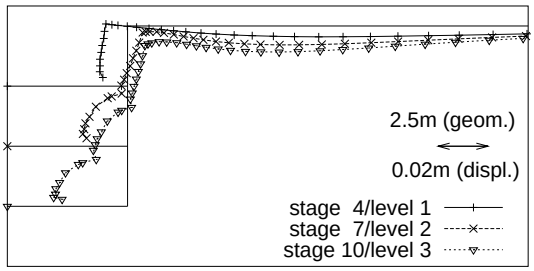

(a) Analyses A and B (stages 4, 7 and 10)

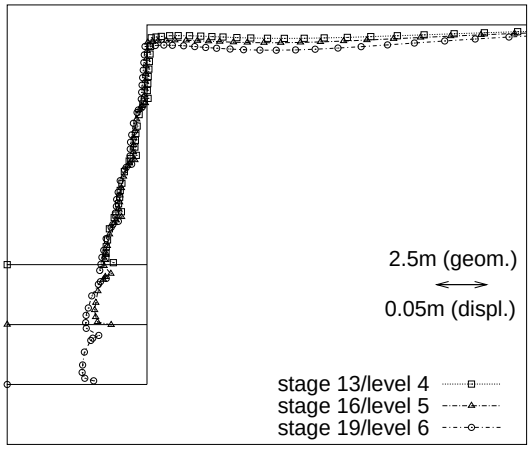

(b) Analysis A (stages 13, 16 and 19)

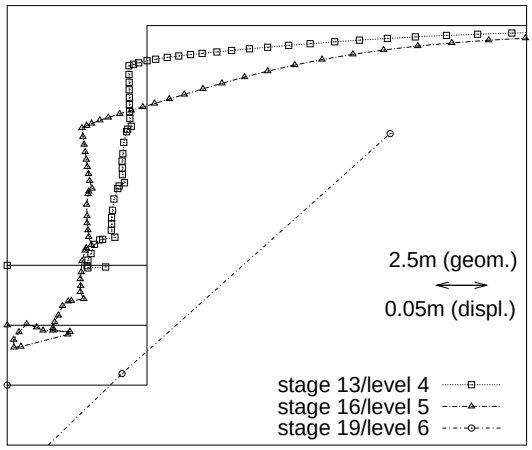

(c) Analysis B (stages 13, 16 and 19)

Figure 7:

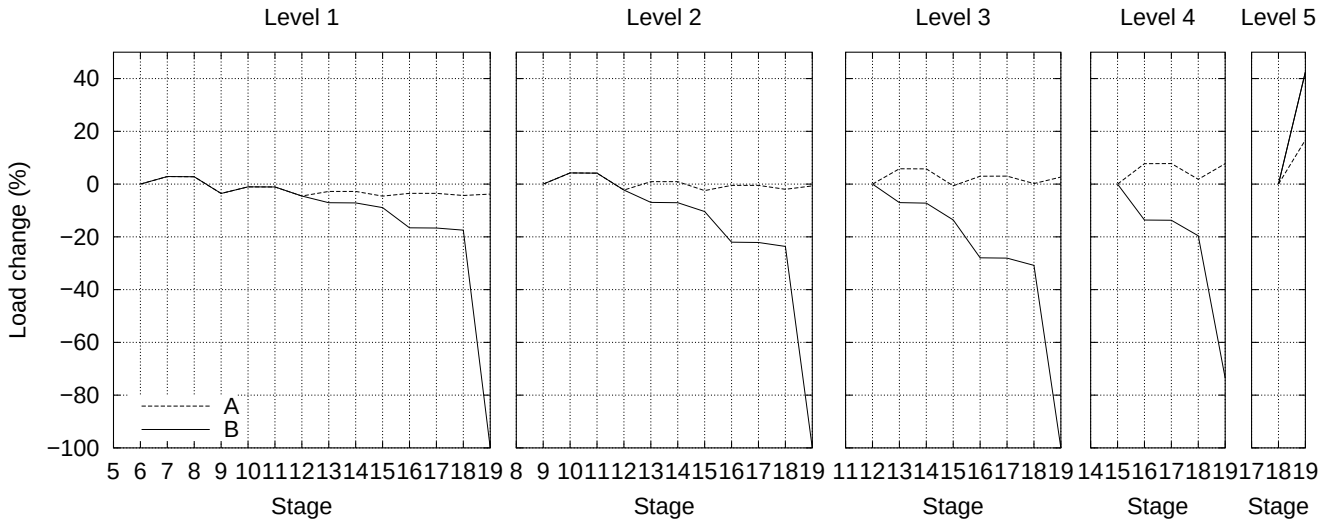
Level 1
Level 2
Level 3
Level 4
Level 5
Load change (%)
40
20
0
−20
−40
−60
−80
−100
A
B
5 6 7 8 9 10 11 12 13 14 15 16 17 18 19
8 9 10 11 12 13 14 15 16 17 18 19
11 12 13 14 15 16 17 18 19
14 15 16 17 18 19
17 18 19
Stage

Figure 8:

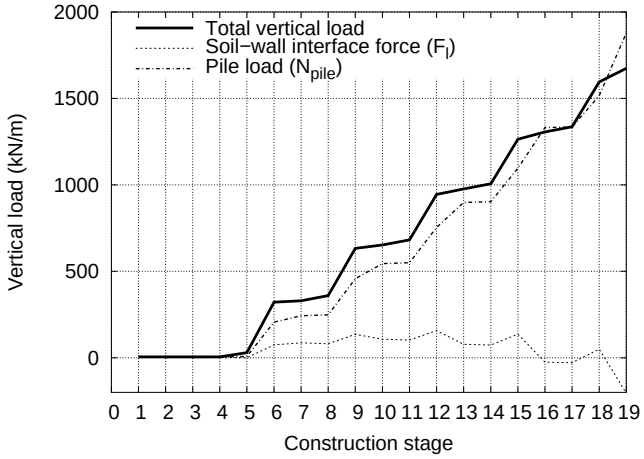

(a) Analysis A

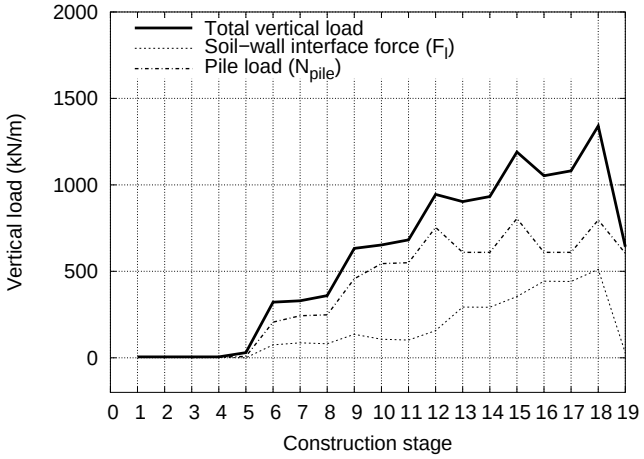

(b) Analysis B

Figure 9:

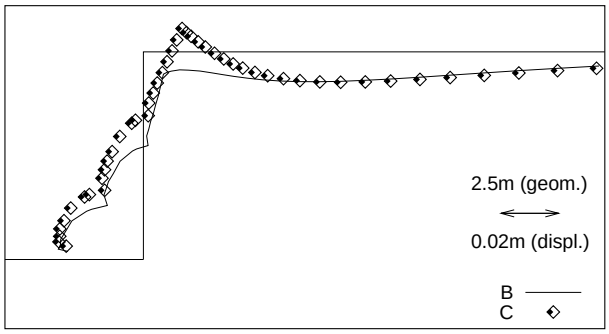

(a) Stage 10

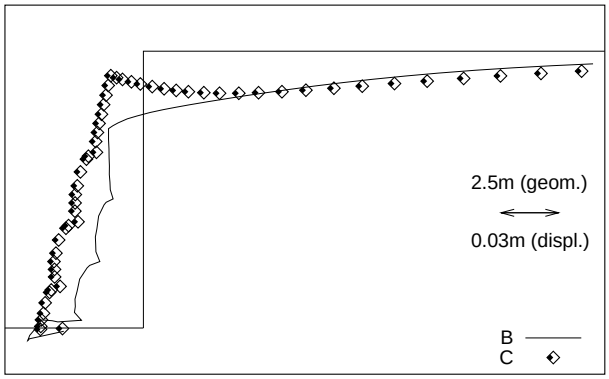

(b) Stage 13

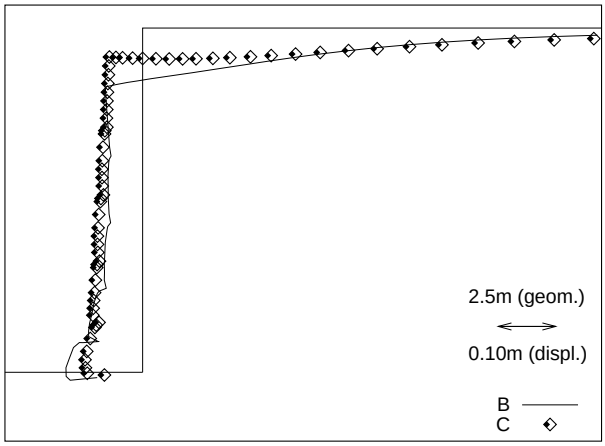

(c) Stage 16

Figure 10:

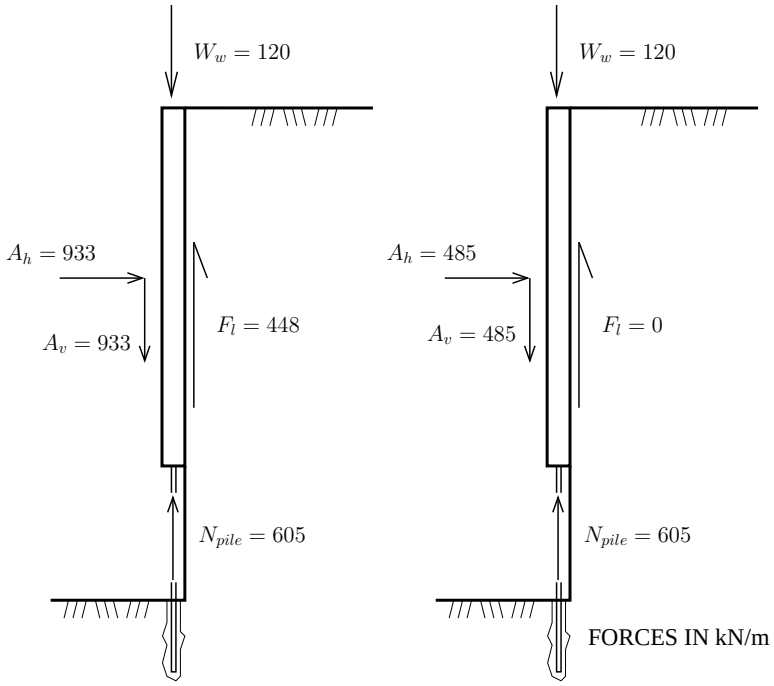

(a) Analysis B

(b) Analysis C

Figure 11:

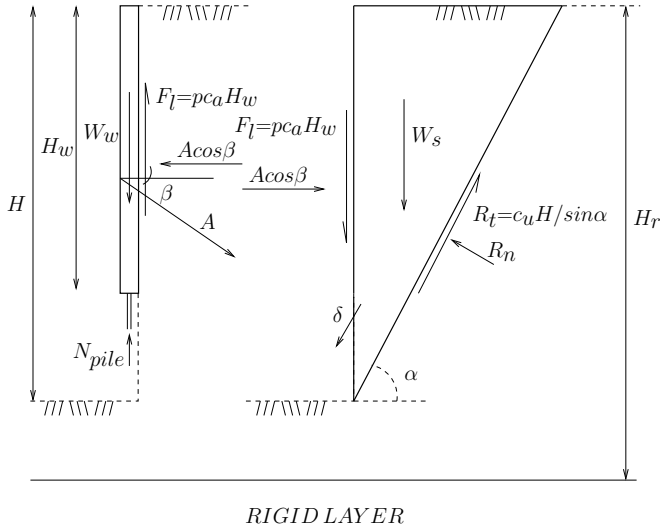
F_l=pc_aH_w
F_l=pc_aH_w
W_w
H_w
$Acos\beta$
$Acos\beta$
β
A
H
W_s
R_t=$c_uH/sin\alpha$
R_n
H_r
δ
N_{pile}
α
$RIGID\ LAYER$

Figure 12:

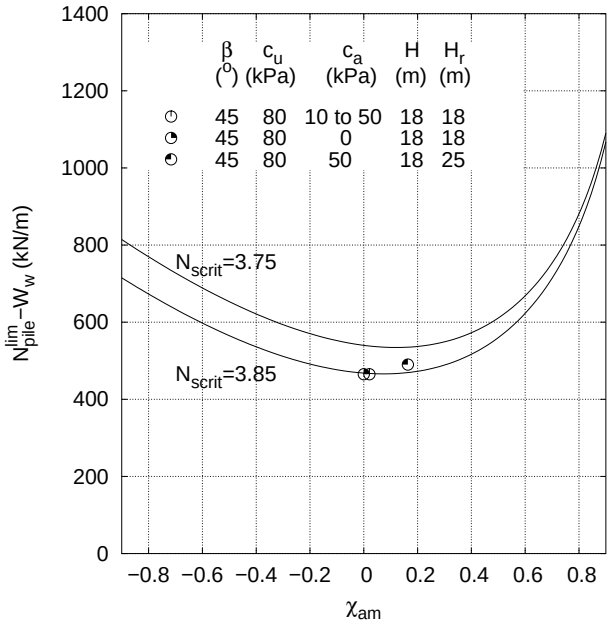
β (°)
c_u (kPa)
c_a (kPa)
H (m)
H_r (m)
45 80 10 to 50 18 18
45 80 0 18 18
45 80 50 18 25
N_{scrit}=3.75
N_{scrit}=3.85
$N^{lim}_{pile}-W_w$ (kN/m)
χ_{am}
1400
1200
1000
800
600
400
200
0
−0.8 −0.6 −0.4 −0.2 0 0.2 0.4 0.6 0.8

Figure 13:

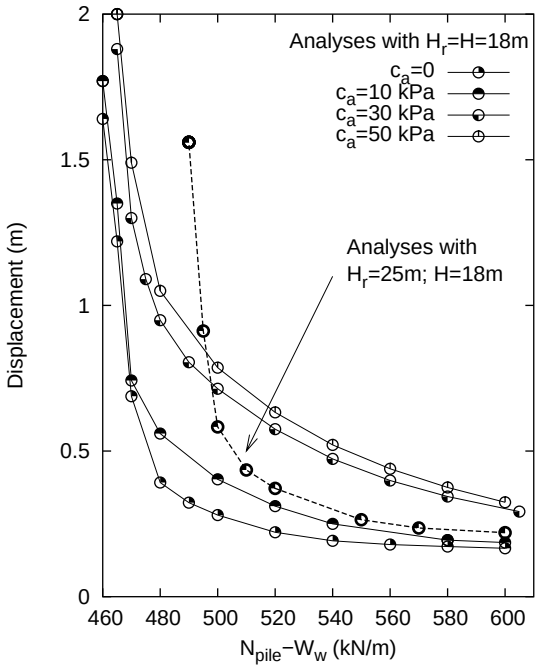
Analyses with H_r=H=18m
c_a=0
c_a=10 kPa
c_a=30 kPa
c_a=50 kPa
Analyses with
H_r=25m; H=18m
Displacement (m)
$N_{pile}-W_w$ (kN/m)
0
0.5
1
1.5
2
460
480
500
520
540
560
580
600

Figure 14:

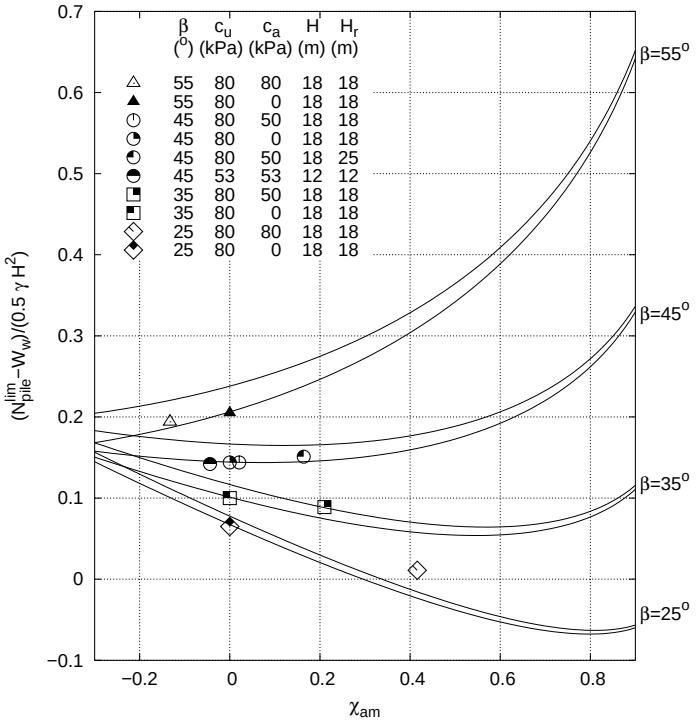
β (°) | c_u (kPa) | c_a (kPa) | H (m) | H_r (m)
55 80 80 18 18
55 80 0 18 18
45 80 50 18 18
45 80 0 18 18
45 80 50 18 25
45 53 53 12 12
35 80 50 18 18
35 80 0 18 18
25 80 80 18 18
25 80 0 18 18
β=55°
β=45°
β=35°
β=25°
$(N_{pile}^{lim}-W_w)/(0.5\ \gamma\ H^2)$
χ_{am}
0.7
0.6
0.5
0.4
0.3
0.2
0.1
0
−0.1
−0.2
0
0.2
0.4
0.6
0.8

Figure 15:

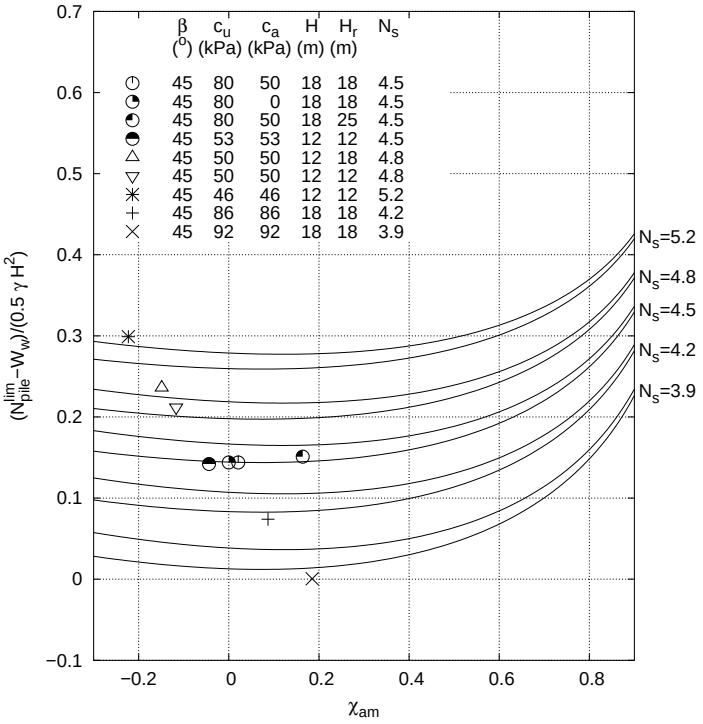
β (°) c_u (kPa) c_a (kPa) H (m) H_r (m) N_s
45 80 50 18 18 4.5
45 80 0 18 18 4.5
45 80 50 18 25 4.5
45 53 53 12 12 4.5
45 50 50 12 18 4.8
45 50 50 12 12 4.8
45 46 46 12 12 5.2
45 86 86 18 18 4.2
45 92 92 18 18 3.9
N_s=5.2
N_s=4.8
N_s=4.5
N_s=4.2
N_s=3.9
(N_pile^lim−W_w)/(0.5 γ H^2)
χ_am
0.7
0.6
0.5
0.4
0.3
0.2
0.1
0
−0.1
−0.2
0
0.2
0.4
0.6
0.8

Figure 16:

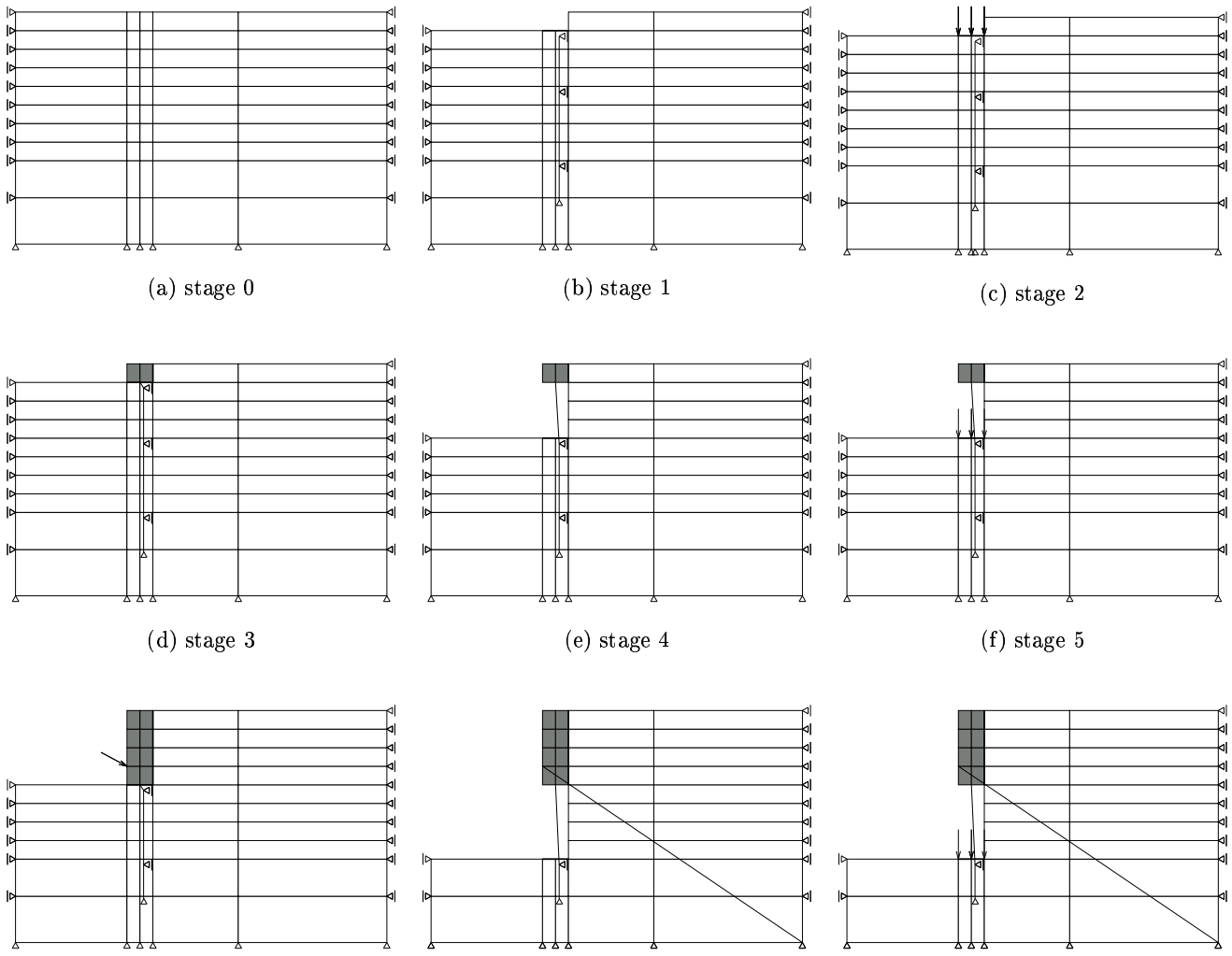

(a) stage 0 (b) stage 1 (c) stage 2

(d) stage 3 (e) stage 4 (f) stage 5

(g) stage 6 (h) stage 7 (i) stage 8

Figure 17:

Figure captions

Figure 1 Construction sequence of a permanent concrete soldier-pile retaining wall.

Figure 2 Vertical stability of concrete soldier-pile walls.

Figure 3 Numerical case study and finite element mesh at the last stage.

Figure 4 Mobilized resistance of the soldier-piles from analysis B.

Figure 5 Shear stresses at the soil-to-wall interface from analyses A and B at stages 10 to 19.

Figure 6 Mobilized resistance of soil-to-wall interface from analyses A and B.

Figure 7 Displacements of the face of the cut and of ground surface for excavation levels 1 to 6 in analyses A and B (note change in scales).

Figure 8 Anchor forces variations in analyses A and B.

Figure 9 Evolution of the vertical resistant forces from analyses A and B.

Figure 10 Displacements of the face of the cut and of ground surface for stages 10, 13 and 16 from analyses B and C (note change in scales).

Figure 11 Forces involved in vertical equilibrium in stage 16 for analyses B and C.

Figure 12 Forces acting on the wall and soil wedge.

Figure 13 Minimum values of pile resistance necessary to avoid soil collapse for N_{scrit} equal to 3.75 and 3.85 ($N_s = 4.5$; $\beta = 45^o$).

Figure 14 Results of finite element calculations: displacement of the upper point of the soil cut in function of the resistance of the piles.

Figure 15 Minimum values of pile resistance necessary to avoid soil collapse for different values of β: theoretical solutions and finite element results ($N_s = 4.5$; N_{scrit} within the range 3.75 to 3.85).

Figure 16 Minimum values of pile resistance necessary to avoid soil collapse for different values of N_s: theoretical solutions and finite element results ($\beta = 45^o$, $N_{scrit} = 3.75$ to 3.85).

Figure 17 Finite element simulation of an excavation supported by a soldier-pile retaining wall.